High-pressure effect on the electronic state in $CeNiGe_3$: pressure-induced superconductivity

2004 J. Phys.: Condens. Matter 16 L255

(http://iopscience.iop.org/0953-8984/16/20/L01)

INSTITUTE OF PHYSICS PUBLISHING JOURNAL OF PHYSICS: CONDENSED MATTER

J. Phys.: Condens. Matter **16** (2004) L255–L262 PII: S0953-8984(04)75804-X

LETTER TO THE EDITOR

High-pressure effect on the electronic state in $CeNiGe_3$: pressure-induced superconductivity

M Nakashima[1,5], K Tabata[2], A Thamizhavel[1], T C Kobayashi[3], M Hedo[4], Y Uwatoko[4], K Shimizu[2], R Settai[1] and Y Ōnuki[1]

[1] Graduate School of Science, Osaka University, Toyonaka, Osaka 560-0043, Japan
[2] Research Center for Materials Science at Extreme Conditions, Osaka University, Toyonaka, Osaka 560-8531, Japan
[3] Department of Physics, Faculty of Science, Okayama University, Tsushimanaka, Okayama 700-8530, Japan
[4] Institute for Solid State Physics, University of Tokyo, Kashiwa, Chiba 277-8581, Japan

E-mail: mnaka@crystal.phys.sci.osaka-u.ac.jp

Received 5 February 2004
Published 7 May 2004
Online at stacks.iop.org/JPhysCM/16/L255
DOI: 10.1088/0953-8984/16/20/L01

Abstract

We have measured the electrical resistivity of an antiferromagnetic Kondo compound $CeNiGe_3$ under pressure. The Néel temperature initially increases with pressure P up to 3 GPa, then decreases rather steeply with further increasing pressure, and becomes zero at a critical pressure $P_c \simeq 5.5$ GPa. The A and ρ_0 values of the resistivity $\rho = \rho_0 + AT^2$ in the Fermi liquid relation become maximum around P_c, the A value attaining an extremely large value which is comparable with that in a heavy fermion superconductor $CeCu_2Si_2$. Superconductivity is found below 0.48 K in a wide pressure region from 4 to 10 GPa. The upper critical field $H_{c2}(0)$ is about 2 T, indicating heavy fermion superconductivity.

In cerium and uranium compounds, the Ruderman–Kittel–Kasuya–Yosida (RKKY) interaction and the Kondo effect compete with each other [1, 2]. The competition between the RKKY interaction and the Kondo effect was discussed by Doniach [3] as a function of $|J_{cf}|D(\varepsilon_F)$, where $|J_{cf}|$ is the magnitude of the magnetic exchange interaction and $D(\varepsilon_F)$ is the electronic density of states at the Fermi energy ε_F. Most cerium compounds order magnetically when the RKKY interaction overcomes the Kondo effect at low temperatures. The magnetic ordering is formed by the localized-4f moments of Ce^{3+}. The topology of the Fermi surface for the conduction electrons is therefore quite similar to that of the corresponding non-4f lanthanum compounds, although the cyclotron mass of the cerium compounds is typically one to two orders of magnitude larger than that of the lanthanum compounds.

[5] Author to whom any correspondence should be addressed.

On the other hand, some cerium compounds such as $CeCu_6$ and $CeRu_2Si_2$ show no long-range magnetic ordering, because the Kondo effect overcomes the RKKY interaction. These compounds are called heavy fermion compounds since they have an extremely large electronic specific heat coefficient γ: $\gamma \simeq 10^4/T_K$ (mJ K^{-2} mol^{-1}), where T_K is called the Kondo temperature: $T_K = 5$ K in $CeCu_6$, for example [1, 2]. In fact, a large cyclotron effective mass of 120 m_0 was detected in the de Haas–van Alphen oscillation in $CeRu_2Si_2$ [4]. Moreover, the topology of the Fermi surface in $CeRu_2Si_2$ is well explained by the 4f-itinerant band model, although the cyclotron effective mass is much larger than the corresponding band mass.

Recently a new aspect of cerium and uranium compounds with magnetic ordering has been discovered. When pressure P is applied to the cerium compounds with antiferromagnetic ordering such as $CeIn_3$ and $CePd_2Si_2$ [5], the Néel temperature T_N decreases, and a quantum critical point corresponding to the extrapolation $T_N \to 0$ is reached at $P = P_c$. Here, $|J_{cf}|D(\varepsilon_F)$ in the Doniach model can be replaced by pressure. Surprisingly, superconductivity appears around P_c. Moreover, a heavy fermion state is formed around P_c, where the non-Fermi liquid nature is also found in some compounds. Similar pressure-induced superconductivity was reported in $CeRh_2Si_2$ [6], $CeRhIn_5$ [7] and UGe_2 [8].

The crossover from the magnetically ordered state to the non-magnetic state under pressure, crossing the quantum critical point, is the most interesting issue in strongly correlated f-electron systems. We have continued studying the effect of pressure on the cerium and uranium compounds [9]. We report in the present work a change of the electronic states in an antiferromagnet $CeNiGe_3$, which is tuned by high pressures up to 10 GPa. The antiferromagnetic Kondo state is changed into the heavy fermion state around a critical pressure $P_c \simeq 5.5$ GPa and becomes a non-magnetic Fermi liquid above P_c. We have found superconductivity around P_c.

There are several intermetallic compounds in the Ce–Ni–Ge system [10–12]: $Ce_3Ni_2Ge_7$ (a Néel temperature $T_N = 7.2$ K), Ce_3NiGe_2 ($T_N = 6.2$ K), $CeNiGe_3$ ($T_N = 5.5$ K) and $Ce_2Ni_3Ge_5$ ($T_N = 4.8$ K). Among them, the magnetic and electrical properties of $CeNiGe_3$ was recently clarified from electrical resistivity, magnetic susceptibility, magnetization, specific heat, neutron powder diffraction and electron diffraction experiments [11, 12]. The crystal structure is the orthorhombic $SmNiGe_3$-type structure (*Cmmm* space group, no. 65), as shown in figure 1. The lattice parameter along the a-axis is extremely large compared to those along the b- and c-axes: $a = 21.808$ Å, $b = 4.135$ Å and $c = 4.168$ Å.

The magnetic susceptibility of a polycrystal sample follows the Curie–Weiss law with an effective moment $\mu_{eff} = 2.58\ \mu_B$/Ce and the paramagnetic Curie temperature $\theta_p = -12$ K. The effective moment is in good agreement with the theoretical value of Ce^{3+}, 2.54 μ_B/Ce. The magnetic susceptibility has a maximum at 5.5 K and decreases with decreasing the temperature, indicating a Néel temperature $T_N = 5.5$ K. The corresponding peak in the specific heat appears at T_N. The magnetic entropy at T_N is estimated as $0.65R \ln 2$, indicating a doublet ground state of the localized 4f-crystalline electric field (CEF) scheme. The electronic specific heat coefficient γ is obtained as 34 mJ K^{-2} mol^{-1}. The electrical resistivity decreases below the Néel temperature.

On the other hand, the neutron powder diffraction experiment indicates a complicated magnetic structure. Two magnetic transitions were observed at $T_N' = 5.9$ K and $T_N'' = 5.0$ K. T_N' is associated with a commensurate collinear antiferromagnetic structure with a propagation vector $\boldsymbol{k}_1 = (100)$, as indicated by arrows in figure 1. The magnetic moments are oriented along the b-axis. On the other hand, T_N'' is associated with an incommensurate antiferromagnetic structure with a propagation vector $\boldsymbol{k}_2 = (0\,0.409\,1/2)$. Below T_N'', the two magnetic structures coexist but the incommensurate structure is highly preponderant. The magnetic moment at the Ce site is determined as 0.8 μ_B/Ce at 1.5 K.

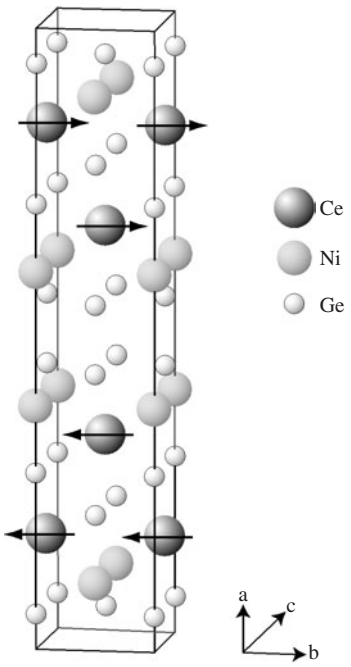

Figure 1. Crystal structure of $CeNiGe_3$. Arrows indicate the magnetic moments corresponding to the propagation vector $\boldsymbol{k}_1 = (100)$.

The present pressure experiments on the electrical resistivity of $CeNiGe_3$ were done by three methods. One is due to an indenter cell in the pressure range from ambient pressure to about 4 GPa in the temperature range from 2 to 300 K. Another is due to a cubic anvil cell at higher pressures up to 8 GPa in the temperature range from 2 to 300 K. The third method is due to a diamond anvil cell at pressures up to 10 GPa in the temperature range from 0.1 to 300 K. The electronic states are tuned by pressure from the antiferromagnetic state to the non-magnetic state, crossing the heavy fermion state in the critical pressure region around 5–6 GPa.

The sample was prepared by arc-melting the stoichiometric amounts of the elements with 3N-(99.9% pure) Ce, 4N-Ni and 5N-Ge under argon atmosphere. The alloy button was wrapped in a Ta-foil, sealed in an evacuated quartz tube and annealed at 800 °C for four days. The residual resistivity ρ_0 and residual resistivity ratio RRR $= \rho_{RT}/\rho_0$ were 1.5 $\mu\Omega$ cm and 220, respectively, indicating a high-quality sample. There are no reports on a single crystal sample of $CeNiGe_3$. We tried to grow a single crystal by the Czochralsky method in a tetra-arc furnace but did not succeed. $CeNiGe_3$ is believed to be an incongruently melting compound.

Figure 2 shows the logarithmic scale of temperature dependence of the electrical resistivity ρ at various pressures, which was obtained by using the indenter cell. The electrical resistivity at ambient pressure has a broad hump around 100 K and also a broad peak around 8 K, and decreases steeply below $T_N = 5.5$ K, which are the same as the previous data [13]. These are characteristic features in the cerium Kondo compound with antiferromagnetic ordering. In cerium Kondo compounds, there are two characteristic Kondo temperatures T_K^h and T_K [14]. For $CeNiGe_3$, T_K^h most likely corresponds to the temperature of 100 K showing the hump, which is named here $T_{\rho max1} = 100$ K, and shown by an arrow in figure 2. T_K roughly corresponds to 8 K, although $CeNiGe_3$ orders antiferromagnetically below $T_N = 5.5$ K. We define the temperature showing the broad resistivity peak as $T_{\rho max2} = 8$ K, as shown by an arrow in figure 2.

With increasing pressure, the electrical resistivity increases in magnitude, and $T_{\rho max1}$ shifts to lower temperatures, while $T_{\rho max2}$ increases with increasing pressure, as shown in figure 2.

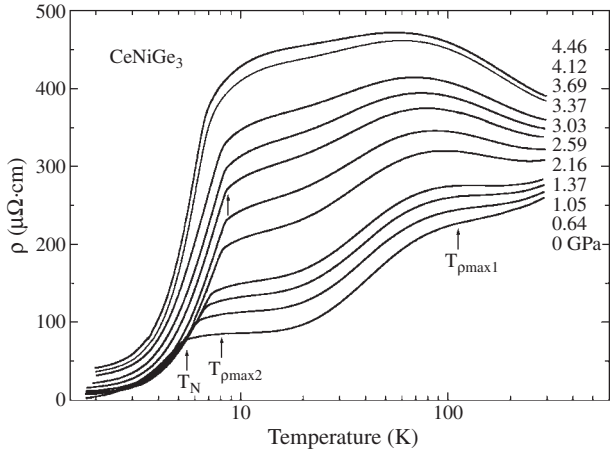

Figure 2. Logarithmic scale of temperature dependence of the electrical resistivity under pressures in $CeNiGe_3$, which was obtained by using the indenter cell. Characteristic temperatures T_N, $T_{\rho max1}$ and $T_{\rho max2}$ are described in the text.

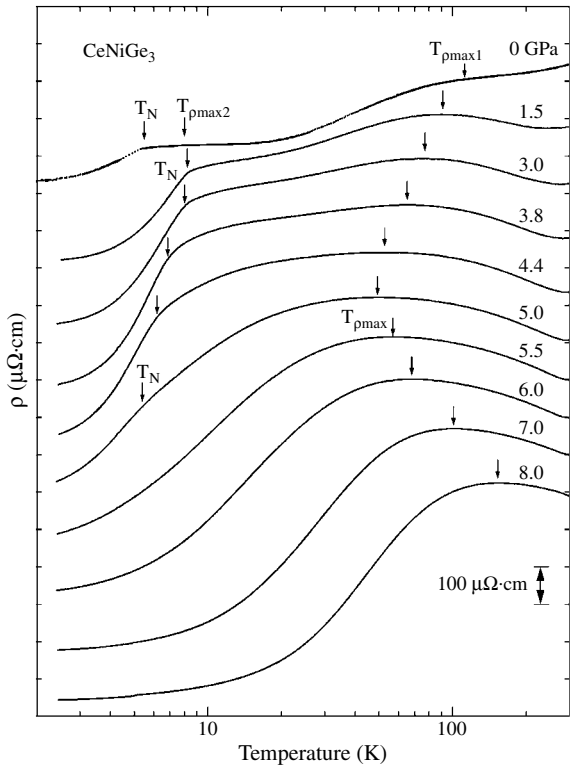

Figure 3. Logarithmic scale of temperature dependence of the electrical resistivity under pressures in $CeNiGe_3$, which was obtained by using the cubic anvil cell.

It is, however, difficult to define $T_{\rho max2}$ above 1 GPa. On the other hand, the Néel temperature increases from $T_N = 5.5$ K at ambient pressure to 8.5 K at 3.03 GPa, as shown by an arrow in figure 2, but decreases with further increasing pressure.

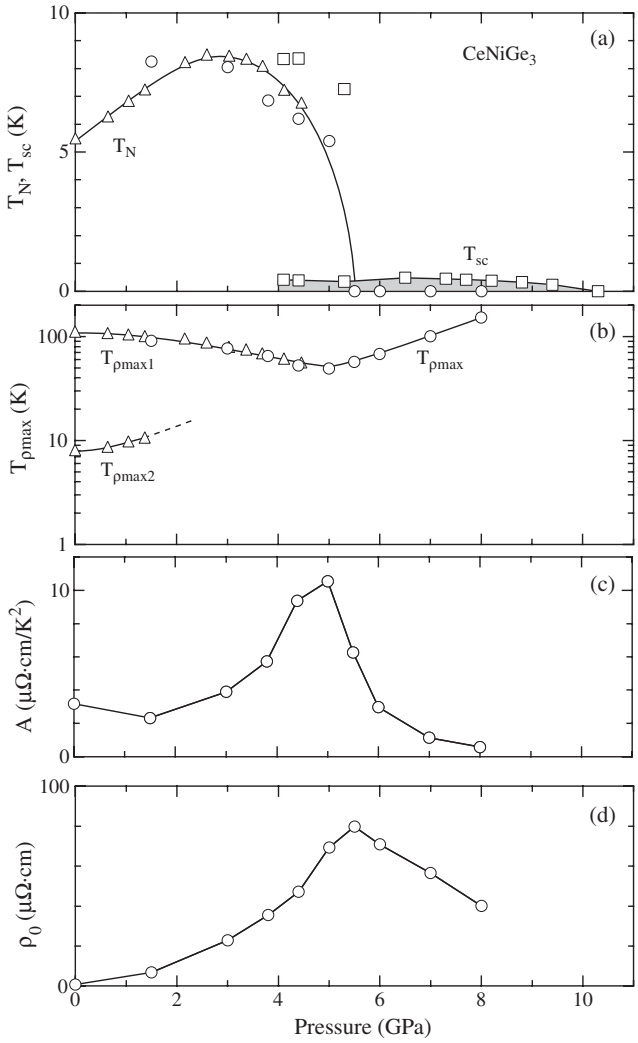

Figure 4. Pressure dependence of T_N, T_{sc}, $T_{\rho max}$, A and ρ_0 values in $CeNiGe_3$. The data shown by triangles, circles and squares were obtained by the indenter, cubic and diamond anvil cells, respectively.

To clarify the behaviour of resistivity at higher pressures, we show in figure 3 the logarithmic scale of temperature dependence of the electrical resistivity at pressures up to 8.0 GPa, which was obtained by using the cubic anvil cell. The resistivity data at different pressures are arbitrarily shifted downwards for simplicity. The two characteristic features at $T_{\rho max1}$ and $T_{\rho max2}$ are found to merge at 5 GPa into a single resistivity peak at $T_{\rho max} = 50$ K. This single resistivity peak at 5 GPa shifts to higher temperatures with further increasing pressure: $T_{\rho max} = 153$ K at 8.0 GPa. The antiferromagnetic ordering most likely disappears at 5.5 GPa. The overall temperature dependence of the electrical resistivity around 5–6 GPa is very similar to that in a heavy fermion superconductor $CeCu_2Si_2$ [15]. On the other hand, the electrical resistivity at 8.0 GPa is typically similar to that observed in a valence fluctuating compound such as CeNi, where the 4f electron is itinerant [16].

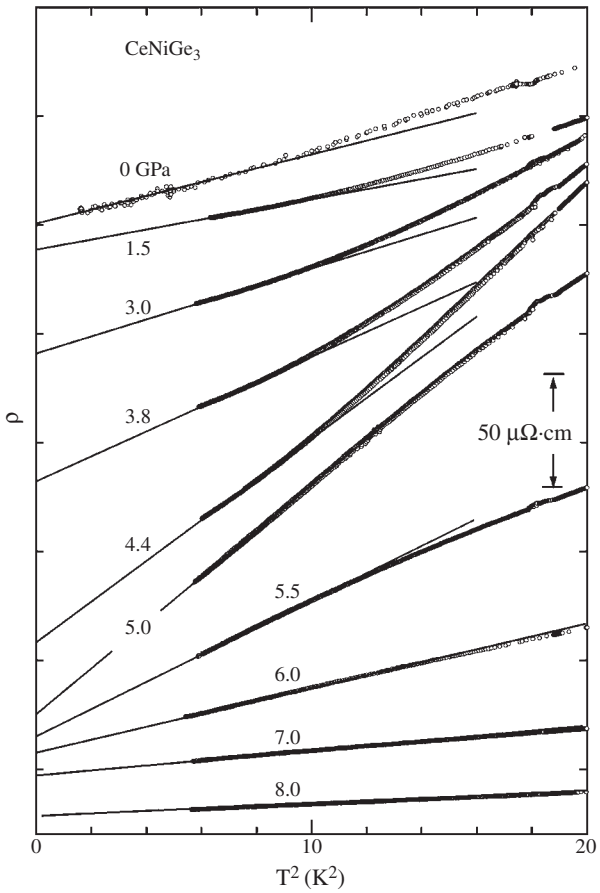

Figure 5. T^2-dependence of the electrical resistivity of $CeNiGe_3$.

Figure 4(a) shows the pressure dependence of the Néel temperature T_N. The data shown by triangles, circles and squares were obtained by using the indenter, cubic and diamond anvil cells, respectively. The data obtained by the diamond anvil cell measurement are described later. Solid lines connecting the data are guidelines. As mentioned above, the Néel temperature attains a maximum at 3 GPa, decreases rather steeply at higher pressures and becomes zero at $P_c \simeq 5.5$ GPa. The two characteristic temperatures $T_{\rho max1}$ and $T_{\rho max2}$ merge into a single characteristic temperature $T_{\rho max}$ above 5 GPa, as shown in figure 4(b).

Here we tried to obtain the A and ρ_0 values from the T^2-dependence of the electrical resistivity at low temperatures, following a Fermi liquid relation, as shown in figure 5. The resistivity data, which were obtained by using the cubic anvil cell, are arbitrarily shifted. Solid lines represent the $\rho = \rho_0 + AT^2$ relation. The A value, which corresponds to the slope of the solid line, becomes maximum around $P_c \simeq 5.5$ GPa, as shown in figures 5 and 4(c). The A value at 5 GPa, 10.5 $\mu\Omega$ cm K^{-2} is the same as 10 $\mu\Omega$ cm K^{-2} in a heavy fermion superconductor $CeCu_2Si_2$ with an extremely large γ value of 1.1 J K^{-2} mol^{-1} [15]. The heavy fermion state is thus formed around $P_c \simeq 5.5$ GPa. Correspondingly, the residual resistivity ρ_0 value also becomes maximum around $P_c \simeq 5.5$ GPa, as shown in figure 4(d).

In order to look for possible superconductivity around P_c, we measured the low-temperature resistivity. Figure 6 shows the temperature dependence of the electrical resistivity at 6.5 GPa under several magnetic fields, which was obtained by using the diamond anvil cell.

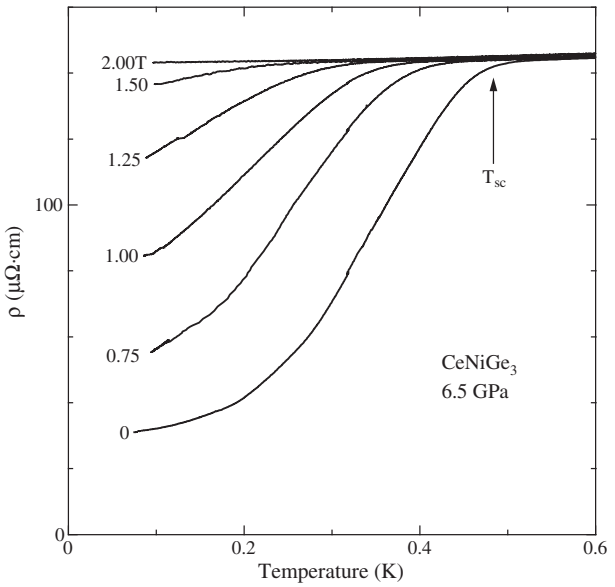

Figure 6. Low-temperature resistivity at 6.5 GPa under several magnetic fields in $CeNiGe_3$.

At zero field, the resistivity decreases rather slowly below 0.5 K. With increasing magnetic fields, the onset of the resistivity drop shifts to lower temperatures and vanishes at $H = 2.00$ T. These results indicate that the present resistivity drop is due to superconductivity. $H_{c2}(0) \simeq 2$ T is consistent with $H_{c2}(0) = 2.0{-}2.4$ T in $CeCu_2Si_2$ [15], together with the A value mentioned above.

We define here the superconducting transition temperature T_{sc} as the onset of the resistivity drop, which is defined as the temperature showing a minimum of $d^2\rho/dT^2$, for example, T_{sc} = 0.48 K at zero field, as shown by an arrow in figure 6.

Figure 7 shows the temperature dependence of the upper critical field H_{c2} at three pressures. The solid curves are guidelines based on the WHH theory [17]. $H_{c2}(0)$ at 6.5 GPa is roughly estimated as 2.0 T, indicating a coherence length $\xi = 130$ Å from $H_{c2} = \phi_0/2\pi\xi^2$, where ϕ_0 is the quantum fluxoid.

We also show in figure 4(a) the pressure dependence of the Néel temperature T_N and the superconducting transition temperature T_{sc} by squares. Superconductivity is observed in a wide pressure region from 4 to 10 GPa in the diamond anvil cell experiment. We note here that the Néel temperature shown by squares is shifted to a higher pressure by about 1 GPa compared to that shown by triangles and circles. Namely, the Néel temperature is 7.3 K at 5.3 GPa and becomes zero at 6.5 GPa in the diamond anvil cell experiment, although the Néel temperature is approximately zero at 5.5 GPa in the cubic anvil cell experiment. This might be due to the fact that pressure is inhomogeneously applied to the sample in the diamond anvil cell compared to the quasi-static pressure in the cubic anvil cell.

The inhomogeneous pressure presumably does not result in a uniform state of superconductivity in the entire sample, as noted for $CeRh_2Si_2$ [18]. This is most likely the cause of the slow drop of the resistivity below T_{sc} and a non-zero resistivity of 30 $\mu\Omega$ cm even at 80 mK under 6.5 GPa, as shown in figure 6. Moreover, the wide superconducting pressure region from 4 to 10 GPa is also related to it. In other words, a true superconducting region might exist in a much narrower pressure region around P_c in which the heavy fermion state is formed.

In conclusion, we have done the experiment of the electrical resistivity under pressure for the antiferromagnet $CeNiGe_3$. The electronic states of $CeNiGe_3$ are thus tuned by pressure

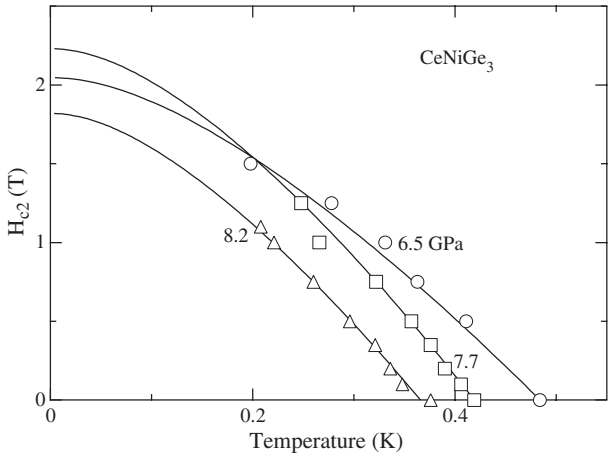

Figure 7. Temperature dependence of the upper critical field H_{c2} at three pressures in $CeNiGe_3$. Solid lines are guidelines.

from the Kondo state with antiferromagnetic ordering to the non-magnetic state (the valence fluctuating state), crossing the heavy fermion state at a critical pressure $P_c \simeq 5.5$ GPa. Superconductivity has been discovered around P_c.

This work was financially supported by the Grant-in-Aid for Creative Scientific Research (15GS0123) and for Scientific Research of Priority Area from the Ministry of Education, Culture, Sports, Science and Technology of Japan.

References

[1] Ōnuki Y, Goto T and Kasuya T 1991 *Materials Science and Technology* vol 3A, ed K H J Buschow (Weinheim: VCH) p 545
[2] Ōnuki Y, Inada Y, Ohkuni H, Settai R, Kimura N, Aoki H, Haga Y and Yamamoto E 2000 *Physica* B **280** 276
[3] Doniach S 1977 *Valence Instabilities and Related Narrow-Band Phenomena* ed R D Parks (New York: Plenum) p 169
[4] Aoki H, Uji S, Albessard A K and Ōnuki Y 1993 *Phys. Rev. Lett.* **71** 2110
[5] Mathur N D, Grosche F M, Julian S R, Walker I R, Freye D M, Haselwimmer R K W and Lonzarich G G 1998 *Nature* **394** 39
[6] Movshovich R, Graf T, Mandrus D, Thompson J D, Smith J L and Fisk Z 1996 *Phys. Rev.* B **53** 8241
[7] Hegger H, Petrovic C, Moshopoulou E G, Hundley M F, Sarrao J L, Fisk Z and Thompson J D 2000 *Phys. Rev. Lett.* **84** 4986
[8] Saxena S S, Agarwal P, Ahilan K, Grosche F M, Haselwimmer R K W, Steiner M J, Pugh E, Walker I R, Julian S R, Monthoux P, Lonzarich G G, Huxley A, Sheikin I, Braithwaite D and Fluquet J 2000 *Nature* **406** 587
[9] Settai R, Araki S, Shishido H, Inada Y, Haga Y, Yamamoto E, Kobayashi T C, Tateiwa N and Ōnuki Y 2003 *J. Magn. Magn. Mater.* **262** 399
[10] Salamakha P, Konyk M, Sologub O and Bodak O 1996 *J. Alloys Compounds* **236** 206
[11] Durivault L, Bourée F, Chevalier B, André G, Weill F and Etourneau J 2002 *Appl. Phys.* A **74** S677
[12] Durivault L, Bourée F, Chevalier B, André G, Weill F, Etourneau J, Martinez-Samper P, Rodrigo J, Suderow H and Vieira S 2003 *J. Phys.: Condens. Matter* **15** 77
[13] Pikul A P, Kaczorowski D, Plackowski T, Czopnik A, Michor H, Bauer E, Hilscher G, Rogl P and Grin Y 2003 *Phys. Rev.* B **67** 224417
[14] Yamada K, Yosida K and Hanzawa K 1984 *Prog. Theor. Phys.* **71** 450
[15] Assmus W, Herrmann M, Rauchschwalbe U, Riegel S, Lieke W, Spille H, Horn S, Weber G, Steglich F and Cordier G 1984 *Phys. Rev. Lett.* **52** 469
[16] Araki S, Settai R, Inada Y, Ōnuki Y and Yamagami H 1999 *J. Phys. Soc. Japan* **68** 3334
[17] Werthamer N R, Helfand E and Hohenberg P C 1965 *Phys. Rev.* **147** 295
[18] Araki S, Nakashima M, Settai R, Kobayashi T C and Ōnuki Y 2002 *J. Phys.: Condens. Matter* **14** L377